KCNE1 and KCNE3 Stabilize and/or Slow Voltage Sensing S4 Segment of KCNQ1 Channel

Koichi Nakajo[1] and Yoshihiro Kubo[1,2,3]

[1]Division of Biophysics and Neurobiology, Department of Molecular Physiology, National Institute for Physiological Sciences, Okazaki, Aichi, 444-8585, Japan
[2]Solution Oriented Research for Science and Technology, Japan Science and Technology Corporation, Kawaguchi, Saitama 332-0012, Japan
[3]COE Program for Brain Integration and its Disorders, Tokyo medical and Dental University, Graduate School and Faculty of Medicine, Bunkyo, Tokyo 113-8519, Japan

KCNQ1 is a voltage-dependent K^+ channel whose gating properties are dramatically altered by association with auxiliary KCNE proteins. For example, KCNE1, which is mainly expressed in heart and inner ear, markedly slows the activation kinetics of KCNQ1. Whether the voltage-sensing S4 segment moves differently in the presence of KCNE1 is not yet known, however. To address that question, we systematically introduced cysteine mutations, one at a time, into the first half of the S4 segment of human KCNQ1. A226C was found out as the most suited mutant for a methanethiosulfonate (MTS) accessibility analysis because it is located at the N-terminal end of S4 segment and its current was stable with repetitive stimuli in the absence of MTS reagent. MTS accessibility analysis revealed that the apparent second order rate constant for modification of the A226C mutant was state dependent, with faster modification during depolarization, and was 13 times slower in the presence of KCNE1 than in its absence. In the presence of KCNE3, on the other hand, the second order rate constant for modification was not state dependent, indicating that the C226 residue was always exposed to the extracellular milieu, even at the resting membrane potential. Taken together, these results suggest that KCNE1 stabilizes the S4 segment in the resting state and slows the rate of transition to the active state, while KCNE3 stabilizes the S4 segment in the active state. These results offer new insight into the mechanism of KCNQ1 channel modulation by KCNE1 and KCNE3.

The Journal of General Physiology

INTRODUCTION

Voltage-gated ion channels are essential for the electrical excitability of neurons, muscles and other excitable cells. Encoded by some 40 different genes and comprised of four six-transmembrane type α subunits, voltage-gated K^+ channels make up the largest family among this group of proteins (Gutman et al., 2005). Hetero-multimeric assembly of the pore-forming α subunits, alternative splicing, and posttranslational modification of the subunits all add to the diversity of the already diverse K^+ channel family (Papazian et al., 1987; Timpe et al., 1988; Isacoff et al., 1990; Ruppersberg et al., 1990; Wang et al., 1998). And still more diversity is added by incorporation of auxiliary subunits into the channel structure (Melman et al., 2002b).

KCNQ1 is a member of the KCNQ (Kv7) voltage-gated K^+ channel subfamily. The properties of the KCNQ1 current, including its gating, single-channel conductance, and expression level, are all markedly altered when the channel associates with one of the KCNE proteins (Barhanin et al., 1996; Sanguinetti et al., 1996; Sesti and Goldstein, 1998; Yang and Sigworth, 1998; Schroeder et al., 2000), a family of five single transmembrane auxiliary proteins for voltage-gated K^+ channels (KCNE1–5) (Takumi et al., 1988; Abbott et al., 1999; Abbott et al., 2001). For example, activation and deactivation kinetics of the KCNQ1 channel are markedly slowed in the presence of KCNE1. KCNQ1 and KCNE1 are endogenously coexpressed in heart and inner ear, and formation of a KCNQ1–KCNE1 complex underlies the slow activation of the delayed rectifier current I_{Ks} (Barhanin et al., 1996; Sanguinetti et al., 1996). Impaired expression of either of their genes causes inherited long QT syndrome (Wang et al., 1996b; Schulze-Bahr et al., 1997; Splawski et al., 1997). Another well-known example is the KCNQ1–KCNE3 complex, which carries the voltage-independent constitutively active K^+ current seen in colon epithelia (Schroeder et al., 2000).

The mechanisms by which KCNE proteins modulate KCNQ1 channel activity are still being debated. Recent biochemical and electrophysiological studies indicate that

Correspondence to Koichi Nakajo: knakajo@nips.ac.jp

The online version of this article contains supplemental material.

Abbreviations used in this paper: DTT, dithiothreitol; MTS, methanethiosulfonate; MTSES, sodium (2-sulfanoethyl) methanethiosulfonate; MTSET, [2-(trimethylammonium)ethyl] methanethiosulfonate bromide.

the transmembrane domain of KCNE1 binds to the pore domain of the KCNQ1 channel (Melman et al., 2004; Panaghie et al., 2006), and it was proposed that direct interaction between KCNE1 and the pore domain of KCNQ1 modulates the channel's gating. With respect to gating, the effects of KCNE1 and KCNE3 are completely opposite; whereas KCNE1 stabilizes a closed state of KCNQ1, KCNE3 stabilizes an open state. Interestingly, these gating properties can be swapped by a single T58V mutation in the transmembrane domain of KCNE1 or a V72T mutation in KCNE3 (Melman et al., 2001, 2002a). On the other hand, the effects of point and deletion mutations in the cytoplasmic C-terminal domain of KCNE1 and KCNE3 suggest that domain also is important for channel modulation (Takumi et al., 1991; Tapper and George, 2000; Gage and Kobertz, 2004). Consistent with that idea, recent identification of the α-helical structure of the cytoplasmic domain of KCNE1 provides a hypothetical site for protein–protein interaction between the cytoplasmic C-terminal domains of KCNE1 and KCNQ1 (Rocheleau et al., 2006).

Although the activation and deactivation kinetics and the voltage dependence of the KCNQ1 channel are all significantly altered by KCNE proteins, little attention has been paid to the function of the S4 segment, which is in the central part of the voltage-sensing domain and could provide clues to understanding KCNE-mediated modulation. One recent report did show that positive charges in the S4 segment play a key role in making KCNQ1 constitutively active when in complex with KCNE3 (Panaghie and Abbott, 2007). How the S4 segment behaves under the influence of KCNE proteins remains largely unknown, however.

State-dependent accessibility analysis using MTS reagents has been applied to assess the movement of the S4 segment in several voltage-gated ion channels (Larsson et al., 1996; Yang et al., 1996; Bell et al., 2004; Vemana et al., 2004). We predicted that if KCNE1 substantially slowed the movement of the voltage sensor (i.e., changed the rate constants), we could detect it as a slower rate of modification. To compare the susceptibility of the KCNQ1 S4 segment to modification in the absence and presence of KCNE proteins, we introduced a series of cysteine substitutions, one at a time, in a region extending from the middle of the S3–S4 linker to the middle of the S4 segment. After some characterization of these mutants, we chose the A226C mutant as the target for MTS modification because it is located at the N-terminal end of S4 segment and its current was stable with repetitive stimuli in the absence of MTS reagent. We estimated that A226C was somewhat buried in the membrane when the channel was in the resting state, but was more exposed to the extracellular milieu during depolarization. Our MTS accessibility data obtained in the presence and absence of KCNE1 suggests that KCNE1 stabilizes the S4 segment in the resting state and reduces the rate of transition to the active state. By contrast, in the presence of KCNE3 the S4 segment loses its state dependence and is stabilized in the active state. We suggest KCNE1 and KCNE3 incline the equilibrium toward the resting and active state, respectively.

MATERIALS AND METHODS

Molecular Biology

Human KCNQ1 (AF000571) and rat KCNE1 (NM_012973) cDNAs were subcloned into the pGEMHE expression vector. Mouse KCNE3 (NM_020574) was obtained by PCR using mouse heart cDNA library and was also subcloned into the pGEMHE vector. Mutations were introduced by PCR using KOD Plus Ver.2 (Toyobo) and confirmed by sequencing. cRNA was then prepared from the linearized plasmid cDNA using an RNA transcription kit (Stratagene).

Preparation of *Xenopus* oocytes

Xenopus oocytes were collected from frogs anesthetized in water containing 0.15% tricaine. After the final collection, the frogs were killed by decapitation. The isolated oocytes were treated with collagenase (2 mg/ml, type 1, Sigma-Aldrich) for 6 h to completely remove the follicular cell layer. Oocytes of similar size at stage V or VI were injected with ∼50 nl of cRNA solution and incubated at 17°C in frog Ringer solution containing (in mM) 88 NaCl, 1 KCl, 2.4 $NaHCO_3$, 0.3 $Ca(NO_3)_2$, 0.41 $CaCl_2$, and 0.82 $MgSO_4$ (pH 7.6) with 0.1% penicillin-streptomycin solution (Sigma-Aldrich). When coexpressing KCNQ1 and KCNE1 or KCNE3, the molar ratio of the mixed RNA was set at ∼10:1. All experiments conformed to the guidelines of the Animal Care Committee of the National Institute for Physiological Sciences.

Two-Electrode Voltage Clamp

2 or 3 d after cRNA injection into KCNE-expressing oocytes and 3–4 d after injection into KCNE-less oocytes, K^+ currents were recorded under two-electrode voltage clamp using an OC725C amplifier (Warner Instruments) and pClamp8 or 10 software (Axon Instruments). Data from the amplifier were digitized at 2 kHz and filtered at 0.2 kHz or digitized at 10 kHz and filtered at 1 kHz. The microelectrodes were drawn from borosilicate glass capillaries (World Precision Instruments) to a resistance of 0.2–0.5 MΩ when filled with 3 M K-acetate and 10 mM KCl (pH 7.2). The bath solution (ND96) contained (in mM) 96 NaCl, 2 KCl, 1.8 $CaCl_2$, 1 $MgCl_2$, and 5 HEPES (pH 7.4). For experiments in Figs. S2 and S3, KD98, which contained (in mM) 98 KCl, 1.8 $CaCl_2$, 1 $MgCl_2$, and 5 HEPES (pH 7.4), and 20K solution, which contained (in mM) 78 NaCl, 20 KCl, 1.8 $CaCl_2$, 1 $MgCl_2$, and 5 HEPES (pH 7.4), were used, respectively. Oocytes held at between −80 and −100 mV were stepped to various test voltages and then to −30 mV to record tail currents (Figs. 1, 2, 6, S1, and S2). Tail current amplitudes were typically measured as the average value 10–20 ms after the end of the test pulse. All experiments were performed at room temperature (25 ± 2°C).

Analysis of Channel Gating

G-V relationships were plotted using tail current amplitudes obtained at −30 mV. Tail currents were fitted using pClamp8 or 10 software to a two-state Boltzmann equation: $G = G_{min} + (G_{max} - G_{min})/(1 + e^{-zF(V - V1/2)/RT})$, where G is determined by the tail current amplitude, G_{max} and G_{min} are the maximum and minimum tail current amplitudes, z is the effective charge, $V_{1/2}$ is the half activation voltage, and T, F, and R have their usual meanings.

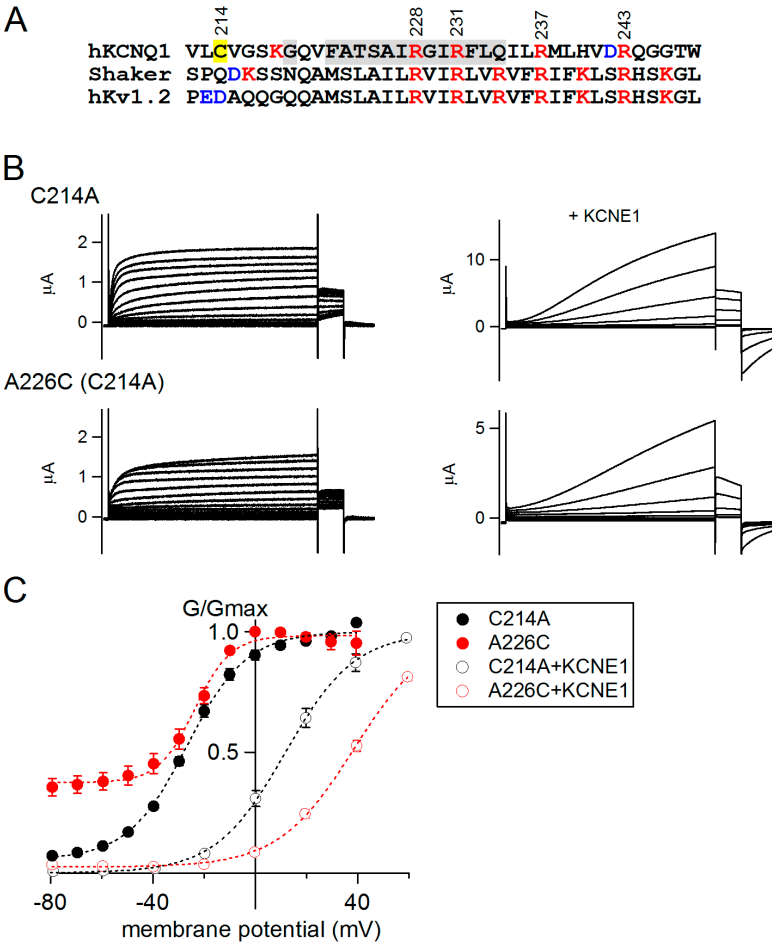

Figure 1. Cysteine-scanning mutagenesis of the S4 segment of the KCNQ1 channel. (A) Amino acid sequences of the S3–S4 linker and S4 segment of human KCNQ1 (hKCNQ1), *Drosophila Shaker* (*Shaker*), and human Kv1.2 (hKv1.2) are aligned. Amino acids substituted with cysteine are shaded in gray. Endogenous cysteine (C214; yellow) was substituted with alanine in all mutants. Positively and negatively charged amino acids are indicated in red and blue, respectively. (B) Representative traces for C214A and A226C in the absence and presence of KCNE1. Membrane potential was depolarized for 2 s from −80 to +40 mV in 10-mV steps in the absence of KCNE1 and from −80 to +60 mV in 20-mV steps in the presence of KCNE1. (C) Conductance–voltage (*G-V*) relationships for C214A (black) and A226C (red) with (open symbols) and without (filled symbols) KCNE1 are shown. Data are fitted with Boltzmann equation (dotted curves, see Materials and Methods).

Analysis of MTS Accessibility

The protocol for the MTS accessibility experiments is shown in Fig. 3 A. The time courses of the MTS reactions were taken as time lapse changes in the instantaneous current amplitude for each depolarization. They were fitted with a single or double exponential function using Igor Pro 5 Software (WaveMetrics, Inc.). The time courses of the modifications were plotted against "exposure (mM s)," which was obtained by multiplying accumulated time of depolarization by the concentration of MTSES (Fig. 3, D and E, and Fig. 4). This definition is based on the assumption that A226C is not accessible to MTSES applied to the external side if the membrane potential is held at −80 mV. This may not be true, however, because A226C was modified by preincubation with MTSET without voltage clamp (Fig. 2; membrane potential was around −60 mV). Nonetheless, the reaction rate seemed to be much faster during depolarization. We assumed that the faster time constant derived from the double exponential function should reflect the reaction rate during depolarization. We therefore employed a faster time constant for the calculation of "apparent" second order rate constants for modification ($s^{-1}mM^{-1}$), which is the inverse of the time constants of modification. The "apparent" second order rate constants for modification were always underestimated because they were mostly measured during the transition of the S4 segment from the resting to the active state, not during the steady active state. And the slower the S4 transition during depolarization, the more underestimated the second order rate constant could be. We compared the "apparent" second order rate constants as parameters reflecting both the accessibility of the target site and the rate of S4 transition.

Drugs

Methanethiosulfonate ethyltrimethylammonium (MTSET) and methanethiosulfonate ethylsulfonate (MTSES) were purchased from Toronto Research Chemicals. They were stored at −20°C and dissolved in the appropriate solution just before use. Once MTS reagent was dissolved, it was always used within 3 h. Dithiothreitol (DTT) was purchased from Promega. DTT was stored as a 100 mM stock solution at −20°C and dissolved in the appropriate solution just before use.

Statistical Analyses

The data are expressed as means ± SEM, with n indicating the number of samples. Differences between means of two groups were evaluated using Student's unpaired t tests. For Fig. 4 B and Fig. 5 E, one- or two-way factorial ANOVA was used for the evaluation. Values of $P < 0.05$ were considered significant.

Online Supplemental Material

The online supplemental material is available at http://www.jgp.org/cgi/content/full/jgp.200709805/DC1. Fig. S1 shows the properties of KCNQ1 cysteine mutants except A226C. Fig. S2 shows reactivities of MTSET on KCNQ1 cysteine mutants except A226C. Fig. S3 demonstrates that MTSES application with 10-s depolarization slows deactivation kinetics of A226C mutant but not of C214A or A226S mutant. Fig. S4 demonstrates that neither C214A nor A226S are reactive to MTSES application, and also shows that current amplitude of endogenous xKvLQT1 is negligible and not reactive to MTSES. Fig. S5 demonstrates that neither C214A nor A226S mutants form disulfide bond with E44C of KCNE1 mutant.

TABLE I

Maximum Tail Current Amplitudes and Parameters of Voltage Dependence for the Cysteine and Serine Mutants Examined in this Study

	Without KCNE1				With KCNE1			
	n	I	$V_{1/2}$	z	*n*	I	$V_{1/2}$	z
		μA	*mV*			μA	*mV*	
Q1 wt	8	0.7 ± 0.1	−24 ± 1	2.4 ± 0.1	5	3.6 ± 0.8	27 ± 3	1.5 ± 0.1
C214A	22	0.9 ± 0.2	−26 ± 1	2.7 ± 0.1	20	8.0 ± 1.3	14 ± 2	1.7 ± 0.1
G219C	16	0.9 ± 0.1	−41 ± 1	1.9 ± 0.1	12	4.5 ± 0.9	16 ± 4	1.6 ± 0.1
F222C	5	0.1 ± 0.0	−10 ± 9	1.5 ± 0.3	9	1.7 ± 0.3	48 ± 4	2.0 ± 0.1
A223C	6	0.5 ± 0.1	−29 ± 6	1.2 ± 0.2	4	1.9 ± 0.9	36 ± 2	1.3 ± 0.2
T224C	6	0.3 ± 0.1	−31 ± 7	1.5 ± 0.3	9	1.7 ± 0.3	26 ± 8	1.2 ± 0.2
S225C	7	0.1 ± 0.0	−26 ± 5	2.0 ± 0.2	9	0.7 ± 0.1	34 ± 6	1.9 ± 0.3
A226C	17	0.4 ± 0.0	−14 ± 3	2.5 ± 0.2	16	3.2 ± 0.3	36 ± 2	1.8 ± 0.1
I227C	4	1.0 ± 0.2	−35 ± 3	2.1 ± 0.2	15	5.4 ± 0.5	−6 ± 4	1.2 ± 0.1
R228C	4	1.1 ± 0.2	53 ± 13	1.5 ± 0.4	7	1.1 ± 0.2	−7 ± 6	1.4 ± 0.2
G229C	12	1.4 ± 0.2	−22 ± 2	2.0 ± 0.1	13	4.2 ± 0.6	9 ± 2	1.5 ± 0.1
I230C	10	2.1 ± 0.4	−30 ± 3	2.1 ± 0.1	18	10.1 ± 1.4	12 ± 3	1.4 ± 0.1
R231C	6	0.1 ± 0.0	−47 ± 2	1.4 ± 0.1	2	0.2 ± 0.0	23 ± 3	1.5 ± 0.0
F232C	17	0.6 ± 0.1	−15 ± 1	2.4 ± 0.2	14	1.5 ± 0.2	−28 ± 3	1.4 ± 0.1
L233C	13	0.8 ± 0.1	−20 ± 1	2.2 ± 0.1	10	4.3 ± 1.0	−4 ± 2	2.0 ± 0.1
Q234C	17	1.1 ± 0.2	−55 ± 1	2.5 ± 0.1	3	10.8 ± 3.6	<−100	ND
A226S	5	0.5 ± 0.1	−14 ± 1	1.7 ± 0.0	5	4.9 ± 1.2	38 ± 2	1.3 ± 0.2

Parameters of voltage dependence were obtained by fitting with Boltzmann equation (see Materials and Methods). Values are means ± SEM. *n*, number of experiments. I, maximal tail current amplitude at −30 mV. $V_{1/2}$ for Q234C+KCNE1 could not be determined because of the extremely negative shift of its *G-V* curve.

RESULTS

Cysteine Scanning Mutagenesis of the Extracellular Side of the S4 Segment

To investigate how the movement of the S4 segment changes in the presence of the auxiliary KCNE proteins, we decided to apply accessibility analysis using MTS reagents (Akabas et al., 1992; Larsson et al., 1996; Yang et al., 1996). To find suitable amino acid residues for this purpose, we introduced cysteine substitutions, one at a time, in a region extending from the middle of the S3–S4 linker through the first half of the S4 segment (Fig. 1 A). There was only one endogenous putative extracellular cysteine, C214. It was substituted with alanine, after which C214A was used as the background for all other mutations. The C214A currents were similar to those carried by wild-type KCNQ1, in both the absence and presence of KCNE1 (Fig. 1 B). All cysteine mutants made in this study were functional and expressible (Table I); however, when arginine residues carrying the positive charges of the S4 segment were substituted (R228C and R231C), the resulting mutants showed very different voltage dependence or very low levels of expression (Table I). Substitution of Q234, which corresponds to the third arginine residue in *Shaker* K^+ channels, also led to a marked shift in the *G-V* curve. Although these three mutants would be interesting to study from the perspective of voltage sensor movement, we generally excluded them from the following analysis. In the absence of KCNE1, the other mutants showed voltage-dependent K^+ currents that were similar to those seen with the wild-type channels (Fig. 1 B and Fig. S1 A, available at http://www.jgp.org/cgi/content/full/jgp.200709805/DC1). The changes induced by KCNE1, including the slowed activation, increased current amplitude, and positive shift of the *G-V* curve, were all conserved in most of the mutants (Fig. 1, B and C, and Fig. S1).

Modification of Cysteine Residues in the S4 Segment by MTS Reagent Makes KCNQ Channels Stabilized in the Open State

Before comparing the rates of the reaction with MTS reagent, we tried to determine which cysteine mutants could be attacked by MTS reagent and what would happen if those cysteine residues were modified. Whether the properties of the K^+ current are altered following MTS modification is largely dependent on the location of the modified cysteine residue. If modification of a particular cysteine residue has an effect on the current, that cysteine is likely located in an important part of the channel. In the present study, we anticipated that all the modifications might have an effect on voltage dependence because all of the exogenous cysteine residues were located within the voltage-sensing domain. If there was no change after the modification, the cysteine in question was presumed to be located in an area that was inaccessible to the MTS, or in a location not important for voltage sensing.

We initially pretreated oocytes expressing both a KCNQ1 cysteine mutant and KCNE1 for 30 min with 1 mM MTSET in ND96 (2 mM K^+). The oocyte was then

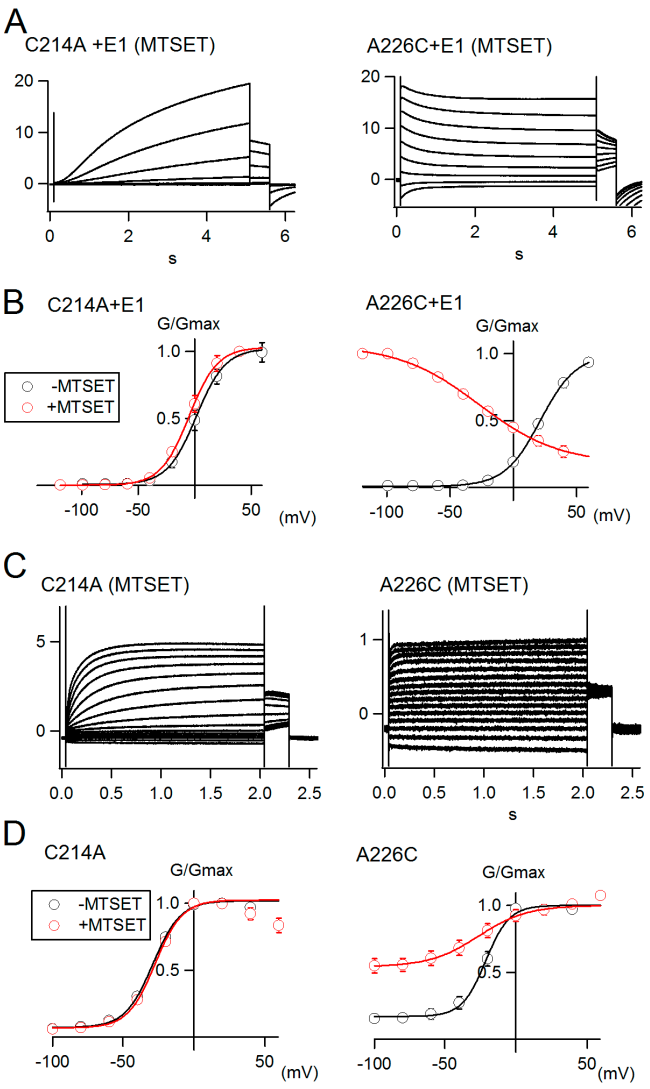

Figure 2. Reaction with MTS reagents locks A226C mutant open. (A) Representative traces for C214A and A226C obtained in the presence of KCNE1 (E1) after a 30-min pretreatment with 1 mM MTSET. A226C was stabilized in the open state after MTSET treatment. Membrane potential was stepped from −120 to +40 mV in 20-mV increments. Holding potential was −90 mV. (B) *G-V* curves with (red) and without (black) MTSET pretreatment in the presence of KCNE1. (C) Representative traces for C214A and A226C obtained in the absence of KCNE1 after a 30-min pretreatment with 1 mM MTSET. Membrane potential was stepped from −100 to +60 mV in 20-mV increments. Holding potential was −80 mV. (D) *G-V* curves with (red) and without (black) MTSET pretreatment in the absence of KCNE1.

recorded in normal ND96 solution to see if there were any changes in the voltage dependence of the channel. Although currents recorded from control oocytes expressing C214A (wild type) and KCNE1 showed no change after MTSET pretreatment, those recorded from oocytes expressing A226C mutant and KCNE1 showed dramatic changes in their voltage dependence following pretreatment with MTSET (Fig. 2, A and B). A226C mutant with KCNE1 was stabilized in the open state,

TABLE II

Summary of State Dependence and Independence of S4 Exposure

	Without KCNE1	With KCNE1
G219C	ND	++
F222C	–	–
A223C	++	++
T224C	++	++
S225C	–	–
A226C	++	++
I227C	ND	++
R228C	+	ND
G229C	+	+
I230C	–	+
R231C	ND	ND
F232C	–	–
L233C	–	–

Qualitative summary of Figs. 2 and S2. ++, always accessible; +, only accessible in 98 mM K^+; –, always inaccessible or modification did not change channel properties.

although a putative inactivating component was seen, and the tail currents somehow became smaller as depolarization became larger. Among the amino acid residues of the S3–S4 linker (G219C, F222C-I227C), the voltage dependences of G219C, A223C T224C, A226C, and I227C were dramatically altered by MTSET pretreatment in the presence of KCNE1 (partly shown in Fig. S2 B). The voltage dependences of G229C, I230C, F232C, and L233C with KCNE1 were not modified by MTSET pretreatment in ND96 (2 mM K^+), but pretreatment made G229C and I230C stabilized in the open state when KD98 (98 mM K^+) was used for the pretreatment (Fig. S2, C and D). In summary, when a KCNQ1 cysteine mutant is coexpressed with KCNE1, MTSET has access to residues 219–227 of the channel in the resting state and to residues 229 and 230 of the channel in the active state (Table II).

Cysteine mutants were also modified by MTSET in the absence of KCNE1. As shown in Fig. 2 (C and D), A226C was modified by MTSET, while the control (C214A) was not, and the modified A226C current was stabilized in the open state (Fig. 2, C and D). As in the presence of KCNE1, the G229C current was only modified in KD98 solution (Fig. S2 E). Only the I230C channel showed a difference in modification depending upon whether or not KCNE1 was present; it was not modified in the absence of KCNE1, even in KD98 solution (Fig. S2, D and E). Thus, although there were some differences, depending on whether or not KCNE1 was present, the range of residues accessible to MTSET appeared to be similar in the resting and active states (summarized in Table II).

Rate of Cysteine Modification was Diminished in the Presence of KCNE1

Among cysteine mutants we created, A226C, I227C, and G229C were good candidates for the purpose of

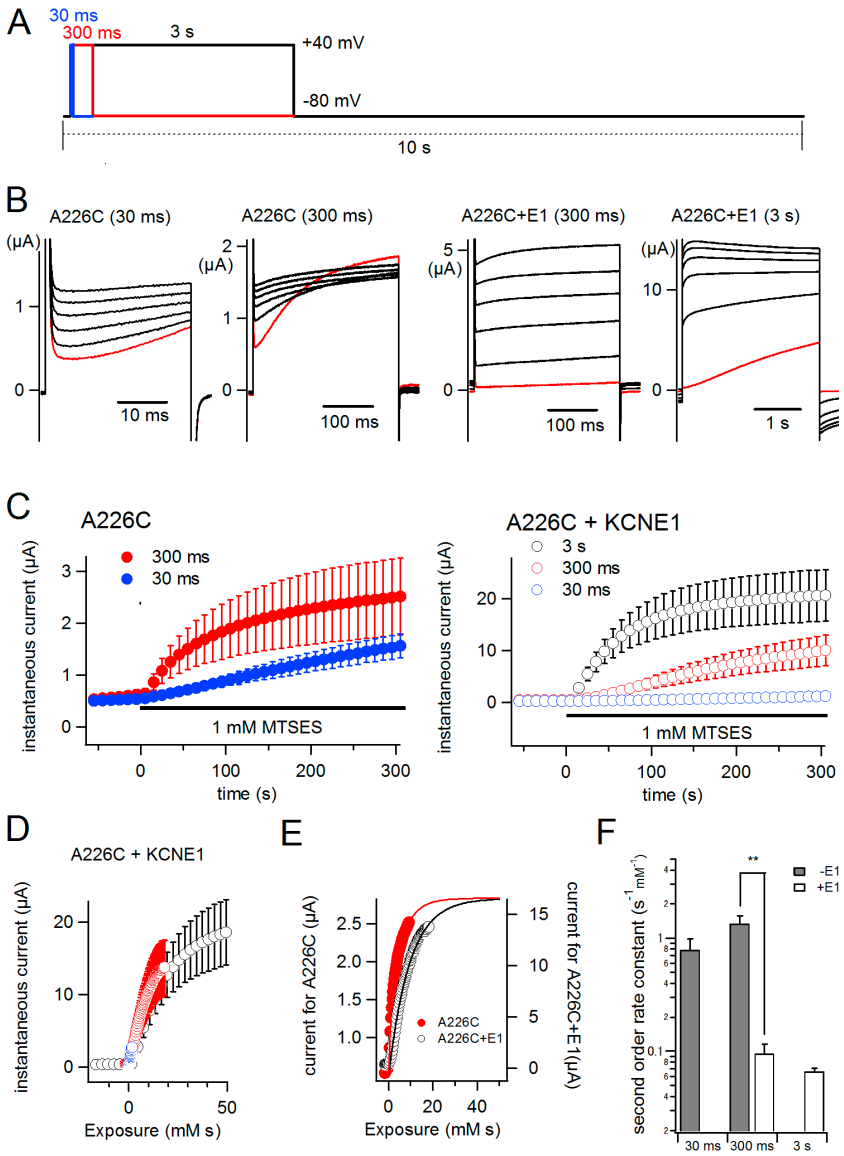

Figure 3. MTS reaction rate is slowed in the KCNQ1–KCNE1 complex. (A) Pulse protocols for MTSES application. Depolarizing pulses (to +40 mV) with durations of 30 ms (blue), 300 ms (red), or 3 s (black) were applied every 10 s. (B) Representative traces for A226C (30 ms), A226C (300 ms), A226C+KCNE1 (300 ms), and A226C+E1 (3 s). Traces obtained just before applying MTSES are shown in red; those obtained 1, 2, 3, 4, and 5 min after the onset of MTSES application are shown in black. (C) Time courses of the MTSES reaction with A226C and A226C+KCNE1 with 30-ms (blue), 300-ms (red), and 3-s (black) depolarizing pulses. The timing of the MTSES application is indicated by black bars. (D) Time courses of MTSES reaction are replotted as functions of "exposure (mM sec)" (see Materials and Methods) of A226C+KCNE1 elicited by 30-ms (blue), 300-ms (red), and 3-s (black) depolarizing pulses. (E) Time courses of the MTSES reaction with 300-ms pulses in terms of "exposure" are compared between A226C and A226C+KCNE1 (E1). Filled red symbols represent A226C, open black symbols A226C+KCNE1. (F) Apparent second order rate constants are plotted. Although time courses of MTSES reaction with A226C (300 ms) and A226C+KCNE1 (3 s) were fitted by a double exponential function, only the faster time constants were used for calculation of the apparent second order rate constants. Filled bars represent rate constants without KCNE1, open bars the rate constants with KCNE1; **, $P < 0.01$.

comparing MTS modification rates. Because they locate at the top of S4 segment, we anticipated that MTS reaction rate for each mutant is voltage dependent. However, as seen in Fig. S1, I227C, especially in the absence of KCNE1, and G229C, especially in the presence of KCNE1, were accumulated in the open state with repetitive depolarization even without MTS reagent probably due to their slow deactivation. In fact, only the A226C current remained stable despite repetitive depolarization, with and without KCNE1 (see Fig. 1 B). In addition, this mutant could be modified by MTS reagent in both the absence and presence of KCNE1 and became stabilized in the open state in either case (see Fig. 2). We therefore chose to use A226C to compare the cysteine modification rates in the absence and presence of KCNE proteins.

Although A226C could be modified by treatment with MTSET in 2 mM K^+ solution for 30 min (see Fig. 2, A and B), we observed that the modification rate was much faster when the membrane potential was depolarized, which means that the S4 segment of A226C is more exposed to the extracellular milieu during depolarization. In this experiment, we used MTSES as the cysteine modification reagent because MTSET can block the pore of the KCNQ1–KCNE1 channel at concentrations in the mM range (Tai et al., 1997). Although MTSES bears a negative charge, while MTSET has a positive charge, currents observed following modification were similarly stabilized in the open state. As shown in Fig. S3, deactivation kinetics of A226C+KCNE1 channel was substantially slowed by 1 mM MTSES with 10-s depolarization while C214A+KCNE1 and A226S+KCNE1 channels were not modified by MTSES. Serine residue, which has a similar molecular radius as cysteine residue but is not MTS reactive, was used for a negative control.

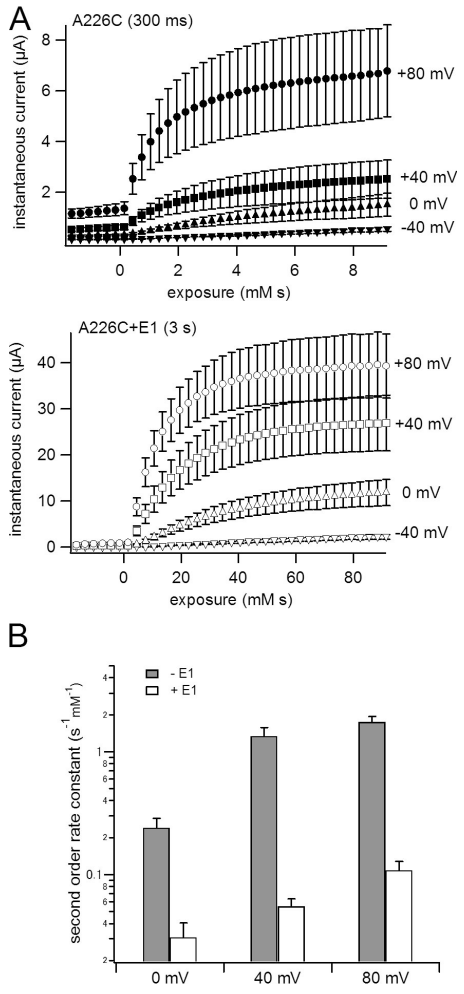

Figure 4. MTS reaction rate is voltage dependent. (A) Time courses of MTSES reaction with A226C (300 ms) and A226C+KCNE1 (3 s) with depolarization to −40, 0, +40, and +80 mV are shown. (B) Apparent second order rate constants are plotted against voltage. Although time courses of the reaction with depolarizations to +40 and +80 mV were fitted with double exponential function, only the faster time constants were used for the calculation of the apparent second order rate constants. Filled bars represent rate constants without KCNE1, open bars the rate constants with KCNE1.

Our protocol entailed applying a depolarizing pulse from a holding potential of −80 to +40 mV for 30, 300, or 3,000 ms every 10 s (Fig. 3 A). We applied 1 mM MTSES between sixth and seventh depolarization. Representative traces recorded just before (red traces) and 1, 2, 3, 4, and 5 min after (black traces) application of MTSES are shown in Fig. 3 B. Longer depolarizing pulses increased the current more quickly in both the absence and presence of KCNE1, which is consistent with our idea that the modification rate is much faster when the membrane potential is depolarized. Notably, the speed of modification was much faster in the absence of KCNE1 (Fig. 3 C). For example, whereas 30-ms depolarizing pulses substantially increased instantaneous current in the absence of KCNE1, they had little effect on KCNQ1 currents when the channel was complexed with KCNE1 (blue symbols in Fig. 3 C). If "exposure" is defined as the duration of depolarization multiplied by the concentration of MTSES, the time course of modification can be plotted as a function of "exposure" (mM s) (Fig. 3, D and E). Fig. 3 D shows that the time course of modification is not dependent on the duration of each depolarizing pulse but on the accumulated depolarization time. Moreover, Fig. 3 E clearly shows that the modification rate is faster in the absence of KCNE1 than in its presence. The time courses for current modification could be fitted with single or double exponential functions. Assuming the faster time constants reflect the rate constant during depolarization, the apparent second order rate constants derived from the faster time constants were 0.8 ± 0.2 (30 ms of KCNQ1; $n = 4$), 1.3 ± 0.2 (300 ms of KCNQ1; $n = 7$), 0.10 ± 0.02 (300 ms of KCNQ1+KCNE1; $n = 9$), and 0.06 ± 0.00 (3 s of KCNQ1+KCNE1; $n = 16$) $s^{-1}mM^{-1}$, respectively (Fig. 3F). Based on the comparison of 300-ms pulses applied in the presence and absence of KCNE1, the rate of modification of KCNQ1 alone was 13 times faster than that of the KCNQ1+KCNE1 complex (P = 0.002, Student's unpaired *t* test).

C214A+KCNE1 and A226S+KCNE1 channels were again not reactive with this repetitive protocol (Fig. S4). We also estimated contamination of potassium current by endogenous *Xenopus* KCNQ1 (xKvLQT1) and exogenous KCNE1. cRNA of KCNE1 at our concentration produced potassium current of <0.3 μA and not reactive to MTSES (Fig. S4). Therefore, contamination of current due to endogenous xKvLQT1 was negligible.

The apparent modification rates should be dependent on the membrane potential during depolarization. To assess the voltage dependence of the modification rate, we applied depolarizing pulses to −40, 0, +40, and +80 mV every 300 ms for A226C alone and every 3 s for the A226C+KCNE1 complex. With both A226C and A226C+KCNE1, the modification rate became faster as the magnitude of the depolarizing potential increased (Fig. 4 A). The calculated apparent second order rate constants for A226C at each membrane potential were 0.24 ± 0.05 ($n = 5$) at 0 mV, 1.3 ± 0.2 ($n = 7$) at 40 mV, and 1.7 ± 0.2 ($n = 5$) at 80 mV, and those for A226C+KCNE1 were 0.03 ± 0.01 $s^{-1}mM^{-1}$ ($n = 5$) at 0 mV, 0.06 ± 0.00 $s^{-1}mM^{-1}$ ($n = 6$) at 40 mV, and 0.11 ± 0.02 ($n = 6$) at 80 mV, respectively (Fig. 4 B). Apparent second order rate constants were voltage dependent and significantly smaller in the presence of KCNE1 (two-way ANOVA, KCNE1 effect, $F_{1,28} = 63.4$, $P < 0.0001$; voltage effect, $F_{2,28} = 12.9$, $P = 0.0001$; KCNE1 × voltage, $F_{2,28} = 10.7$, $P = 0.0004$). These differences in the apparent rate constants probably reflect the slow transition of the S4 segment in the presence of KCNE1. Notably, the rate constant for A226C at 0 mV (0.24 ± 0.05 $s^{-1}mM^{-1}$)

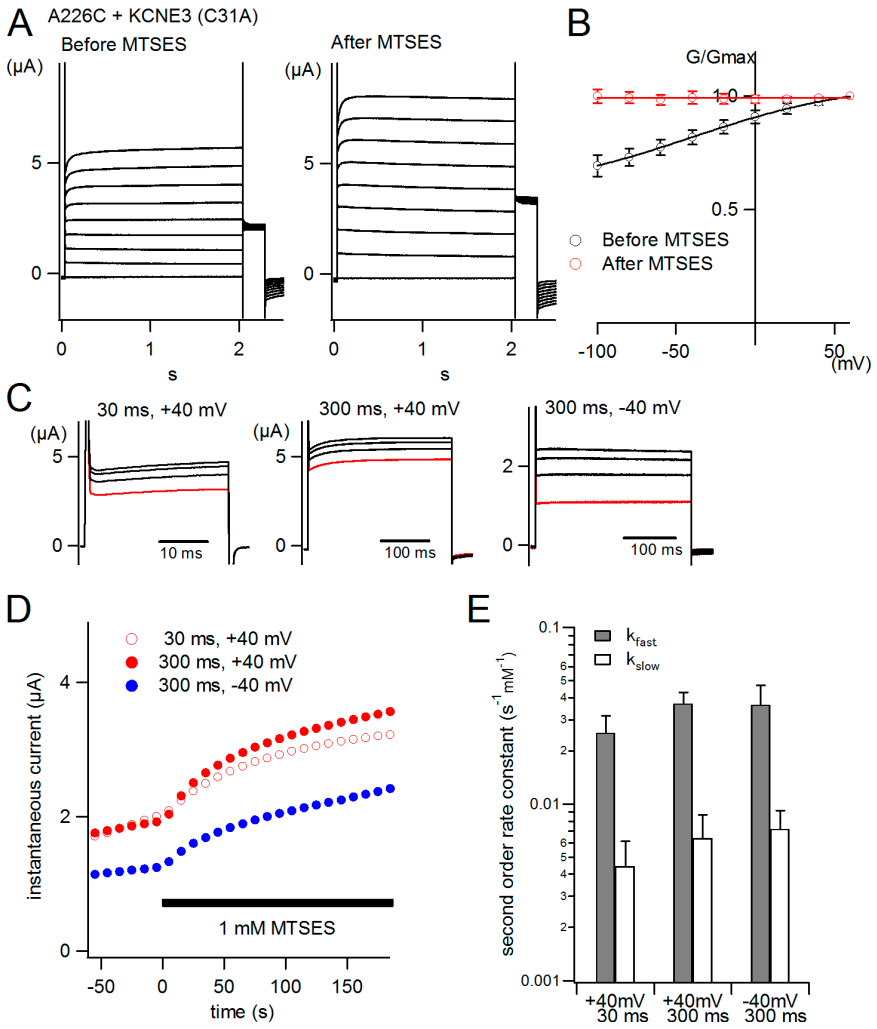

Figure 5. The rate of MTS reaction with the KCNQ1–KCNE3 complex is voltage independent. (A) Representative traces obtained from oocyte coexpressing KCNQ1 (A226C) and KCNE3 (C31A) before and 5 min after application of 1 mM MTSES. Membrane potential was stepped from a holding potential of −100 to +60 mV in 20-mV increments. (B) *G-V* relationships for A226C+KCNE3 before (black) and after (red) MTSES application. (C) Representative traces obtained with 30-ms depolarizations to +40 mV or 300-ms depolarizations to +40 or −40 mV in oocytes expressing A226C+KCNE3. Traces just before applying MTSES are shown in red; those recorded 1, 2, and 3 min after the onset of MTSES application are shown in black. (D) Time courses of the MTSES reaction with A226C+KCNE3. Error bars were omitted for clarity. The timing of MTSES application is indicated by a black bar. (E) Two second order rate constants (k_{fast} and k_{slow}) are plotted for each protocol. They are calculated from two time constants obtained from D fitted using a double exponential function.

is comparable with A226C+KCNE1 at +80 mV (0.11 ± 0.02 $s^{-1}mM^{-1}$). Because this voltage gap is even larger than the *G-V* shift induced by KCNE1 (50 mV in A226C mutant; see Fig. 1 C and Table I), the slow rate induced by KCNE1 cannot be explained simply by the voltage dependence shift seen in *G-V* curve. Instead, these results support the idea that the rate of transition of the S4 segment to the activation state is strongly reduced by KCNE1.

Rate of Cysteine Modification of A226C Is Not State Dependent in the Presence of KCNE3

KCNE3 is another auxiliary subunit for KCNQ1. Both KCNQ1 and KCNE3 are coexpressed in small intestine and colon, where they form a constitutively open K^+ channel (Schroeder et al., 2000). We were interested in seeing how the S4 segment behaves within the KCNQ1–KCNE3 complex. KCNE3 has an endogenous cysteine residue in the extracellular N-terminal domain. We substituted that cysteine with alanine (C31A) and then used this KCNE3 mutant for experimentation. Coexpression of KCNQ1 (A226C) and KCNE3 (C31A) produced K^+ channels that were nearly entirely constitutively open (Fig. 5 A). They still remained slightly voltage dependent, but that voltage dependence disappeared almost completely after the application of 1 mM MTSES (Fig. 5 B). Current amplitude was also somewhat enhanced after application of MTSES (Fig. 5 A), which enabled us to detect the modification process. After application of 1 mM MTSES, current amplitude increased as shown in Fig. 5 C. Interestingly, the time courses of modification were not dependent on the duration or the amplitude of the depolarizing pulse (Fig. 5 D), which suggests that in the presence of KCNE3 the C226 residue is accessible to MTSES, almost irrespective of membrane potential. The time courses of the modification were fitted with a double exponential function from which two apparent second order rate constants (k_{fast} and k_{slow}) were obtained. To calculate k_{fast} and k_{slow}, we assumed that the C226 residue was always exposed to the extracellular milieu and employed total time instead of depolarizing time. The values for k_{fast} were 0.025 ± 0.006 (40 mV, 30 ms; $n = 8$), 0.037 ± 0.006 (40 mV, 300 ms; $n = 11$), and 0.037 ± 0.010 $s^{-1}mM^{-1}$ (−40 mV, 300 ms; $n = 8$), while

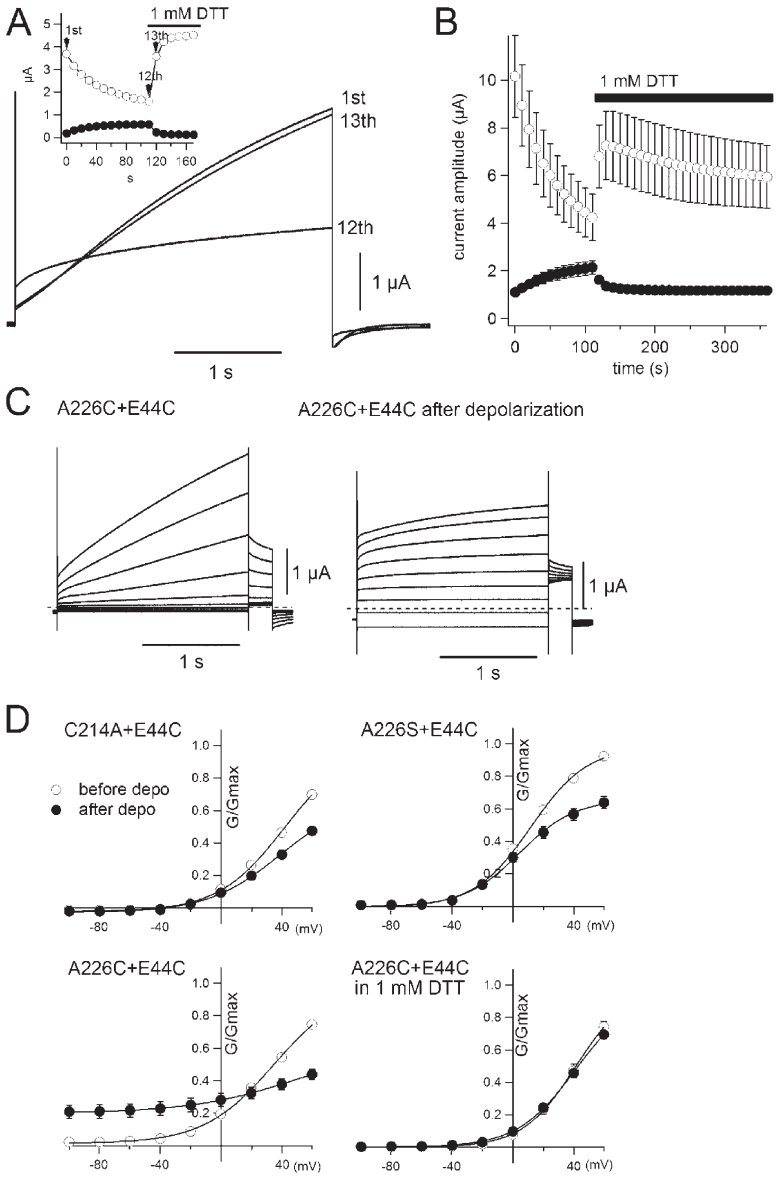

Figure 6. A disulfide bond can form between KCNE1 and S4 of KCNQ1. (A) Current traces recorded from an oocyte coexpressing KCNQ1 (A226C) and KCNE1 (E44C) are shown. The oocyte was repetitively depolarized to +40 mV for 3 s every 10 s. Only the 1st, 12th, and 13th traces are shown. The current gradually ran down until by the 12th depolarization it was nearly flat. With subsequent addition of 1 mM DTT, the current immediately recovered the slow activation (13th depolarization). Thereafter, slow activation was retained in DTT. (inset) Time course of the run down and recovery by DTT. Filled and open symbols represent the instantaneous currents and the currents at the end of the depolarization, respectively. Black bar represents the presence of 1 mM DTT in the bath solution. (B) Time course of current amplitude upon DTT application ($n = 5$). Filled and open symbols represent the instantaneous currents and the currents at the end of the depolarization, respectively. Black bar represents the presence of 1 mM DTT in bath solution. (C) Representative traces obtained from oocyte coexpressing KCNQ1 A226C mutant and KCNE1 E44C mutant. Membrane potential was stepped from a holding potential of −100 to +60 mV in 20-mV increments. After the first set of voltage pulses (left), oocyte is depolarized at +40 mV for 1 min to facilitate the disulfide formation. Second set of voltage pulses was applied after 1 min depolarization (right). (D) *G-V* curves for the KCNQ mutants with KCNE1 (E44C) mutant. Open and filled symbols represent *G-V* curves before and after 1 min depolarization at +40 mV, respectively.

those for k_{slow} were 0.004 ± 0.002 (40 mV, 30 ms), 0.006 ± 0.002 (40 mV, 300 ms), and 0.007 ± 0.002 $s^{-1}mM^{-1}$ (−40 mV, 300 ms), respectively (Fig. 5 E). Clear voltage or pulse duration dependence were not seen from k_{fast} (one-way ANOVA, $F_{2,24} = 0.73$, $P = 0.49$). It thus appears that KCNE3 stabilizes the S4 segment at a position in which C226 is continuously accessible.

The Position of KCNE1 Is Close Enough to Form a Disulfide Bond with the S4 Segment

It has been reported that KCNE1 binds directly to the KCNQ1 pore domain (Tapper and George, 2001; Melman et al., 2004; Panaghie et al., 2006). According to the recent structural data for the Kv1.2 channel (Long et al., 2005), there is a large gap between the two neighboring voltage-sensing domains in the channel (S1 and S4). If KCNE1 could fit into that gap, it could interact with both the S4 segment and the pore domain. To determine if this is the case, we introduced a cysteine mutation at E44 of KCNE1, which is located just above the transmembrane domain. E44 appears to be exposed to the extracellular milieu, as it is accessible to extracellular MTSES, which can then block the channel pore (Wang et al., 1996a). When the E44C KCNE1 mutant was coexpressed with the A226C KCNQ1 mutant, the resultant complex showed a slowly activating K^+ current just like the wild-type KCNQ1–KCNE1 complex (Fig. 6 A, first trace). When we applied 3-s depolarizing pulses to +40 mV every 10 s, current amplitude at the end of the pulse (open circles) gradually declined, but instantaneous current (filled circles) increased (Fig. 6, A and B). The current continued to lose its slowly activating component and eventually became close to flat (Fig. 6 A, 12th trace). When we then applied a reducing agent

(1 mM DTT), current instantaneously returned to the initial state and again showed slow activation (Fig. 6 A, 13th trace). In the presence of DTT, the instantaneous current never increased, and the slow activation was retained. Current amplitudes of C214A or A226S with E44C were relatively stable during repetitive depolarization and DTT application (Fig. S5). These results imply that disulfide bonds gradually formed during the repetitive depolarization and that these bonds restricted the movement of the S4 segment within the channel. Similar observations were also obtained by a different protocol. Between two sets of voltage pulses from −100 to +60 mV, oocytes were held at +40 mV for 10 s to facilitate the formation of disulfide bonds. As shown in Fig. 6 C, A226C+E44C channels became stabilized in the open state after the depolarization. Neither C214A+E44C channels nor A226S+E44C channels became stabilized in the open state after the depolarization, and 1 mM DTT prevented A226C+E44C channels from being stabilized in the open state (Fig. 6 D). These results suggest that C44 of the KCNE1 mutant was close enough to form a disulfide bond with C226 in the S4 segment of the KCNQ1 mutant and supports the hypothesis that KCNE1 directly interacts with the S4 segment to regulate voltage-sensing function.

DISCUSSION

The voltage dependence of the KCNQ1 channel is markedly altered in the presence of KCNE auxiliary proteins (Barhanin et al., 1996; Sanguinetti et al., 1996; Schroeder et al., 2000). Our aim in the present study was to determine how the movement of the voltage-sensing S4 segment is affected by the presence of KCNE1 or KCNE3. We will discuss the likely meaning of our findings from the viewpoint of the channel modification by the auxiliary subunits.

What Slows the Activation of KCNQ1–KCNE1 Current?

Our present results using MTS regents suggest that S4 movement in KCNQ1–KCNE1 complex is substantially slowed by the presence of KCNE1. Is slow movement of S4 segment the rate-limiting step in activation of KCNQ1–KCNE1 complex?

There have been several reports claiming that KCNE1 is close to the conduction pathway (Wang et al., 1996a; Tai and Goldstein, 1998; Kurokawa et al., 2001; Tapper and George, 2001) and directly binds to the pore domain or S6 segment (Melman et al., 2004; Panaghie et al., 2006). That direct interaction between KCNE1 and the pore/S6 segment of KCNQ1 has been considered to play a role in modulating the channel's gating. If the movement of S6, which comprises gating hinge (Seebohm et al., 2006), is substantially slowed by the KCNE1 interaction, this step can be a rate-limiting step in activation and deactivation. On the other hand, less attention has been paid to the S4 movement in KCNQ1–KCNE1 complex and the possible role for S4 segment in KCNQ1 modulation. However, a recent study by Panaghie and Abbott (2007) showed that S4 charges are crucial to the gating modulation by KCNE proteins. Their study strongly suggests that KCNE proteins, directly or indirectly, interact with S4 segment of KCNQ1 channel. In addition, as shown in Fig. 6 in our present study, E44C in KCNE1 could make a disulfide bond with A226C in S4 segment of KCNQ1 during depolarization. Our result proposes the proximity and possible direct interaction between S4 segment and KCNE1. Nonetheless, it is still equally possible that KCNE1 and KCNE3 interact with pore domain or other structures that indirectly modulate S4 movement.

Generally, voltage-gated ion channels show current having some sigmoidicity at the beginning of activation due to the independent movement of four S4 voltage sensors. However, in two *Shaker* mutants, Shaw S4 mutant and ILT mutant, activation kinetics can be fitted with a single exponential function because the final voltage-dependent cooperative step is slowed and becomes a rate-limiting step in these mutants (Smith-Maxwell et al., 1998a,b; Ledwell and Aldrich, 1999). If S6 movement or final gating step is slowed by KCNE1 and is the rate-limiting step, activation should be fitted with a single exponential function and sigmoidal activation should not be seen. However, current by KCNQ1–KCNE1 complex shows clear sigmoidicity (see Fig. 1 B), suggesting S4 movement may be the rate-limiting step in activation.

Because of the limitation of MTS experiments, we did not investigate the slow deactivation in KCNQ1–KCNE1 complex. In this case, deactivation kinetics of KCNQ1–KCNE1 complex can be fitted with a single or double exponential function (unpublished data), therefore S6 movement (or final gating step) could be a rate-limiting step. Further experiments are required for claiming which part is responsible for the slow deactivation of KCNQ1–KCNE1 complex.

How Does the Voltage-sensing Domain of KCNQ1 Behave Under the Influence of KCNE1?

The results summarized in Fig. S2 and Table II show that the range of accessibility of the voltage sensor does not differ much in the presence and absence of KCNE1. A226 and I227, the amino acid residues above the first arginine (R228) are accessible from the extracellular milieu although the accessibility is quite small at hyperpolarized potential. In contrast, G229 and I230, situated between the first and second arginine (R231), are exposed to the extracellular milieu only when the membrane is depolarized, and the amino acid residues below R231 (F232, L233, and Q234) are inaccessible to the extracellular MTS reagents. This profile is similar to that of the *Shaker* K^+ channel, in which the first arginine

(R362) is accessible from the outside regardless of the channel state, and the second arginine (R365) becomes accessible from the outside when the channel is in the open state (Larsson et al., 1996).

On the other hand, the rates of the MTSES reaction with A226C differed considerably in the presence and absence of KCNE1. When KCNE1 was present, the apparent second order rate constant was 13 times slower than when it was absent (Fig. 3). What does this result mean? Because the activation kinetics of the KCNQ1+KCNE1 current is extremely slow, a steady state is not reached even with a depolarizing pulse 3 s in length. If the slow activation kinetics directly reflect the slow movement of the voltage sensor, the S4 segment may be in a transition to a new equilibrium rather than in a steady state during the short depolarizing pulses (30–3,000 ms) applied in this study. Therefore, MTS accessibility to S4 of the KCNQ1+KCNE1 channel should reflect the transition rate of the S4 segment rather than the degree of exposure of the S4 segment in the steady state. KCNQ1 without KCNE1 reaches a steady state during 1-s depolarizing pulses, but is probably in the transition to a new equilibrium during 30- or 300-ms pulses. Consequently, what we measured and compared in Figs. 3 and 4 is related not only to the rate constant for modification in the active state, but also to the rate constant of the transition of the S4 segment from the resting state to the active state. Thus our interpretation for the slowed reaction rate in the presence of KCNE1 is that the rate of transition of the S4 segment from the resting state to the active state is diminished in the presence of KCNE1.

We considered the possibility that our results are explained merely by the shift in the voltage dependence of the S4 segment because the A226C mutant shows a large positive shift in its *G-V* curve (50 mV) in the presence of KCNE1 (Fig. 1 C). However, we think that is unlikely because such a scenario cannot explain the observation that the apparent second order rate constant for the KCNQ1+KCNE1 channel at +80 mV is comparable with that of KCNQ1 at 0 mV (Fig. 4). Another possible explanation for the slowed reaction rate is that KCNE1 protects the C226 site and prevents MTS reagents from accessing it. To exclude this possibility, we may need a more direct method of observing the voltage sensor movement, for example fluorometric analysis using tetramethylrhodamine maleimide (Mannuzzu et al., 1996).

At a certain voltage, transition of the S4 segment from the resting state to the active state is dependent on the total duration of the depolarization because the time courses of the current development induced by MTSES are overlapped among protocols with different pulse durations (Fig. 3 D). This implies that the transition of the voltage sensor may be governed by one rate-limiting step, in at least a 30-ms time window. Once the membrane is depolarized, there is a certain probability that the voltage sensor will go into the active state in a single step. And this probability may be 13 times lower in the presence of KCNE1.

How Does the Voltage-sensing Domain of KCNQ1 Behave Under the Influence of KCNE3?

In the presence of KCNE3, KCNQ1 is constitutively open, regardless of voltage. There are two possible explanations for this constitutive activation: KCNE3 may lock the gate in an open state and uncouple it from the movement of the S4 segment or it may lock the S4 segment in the active state. Panaghie and Abbott (2007) showed that the proportion of constitutively active channels is altered by substituting alanine for basic residues. If KCNE3 uncouples the gate from the S4 movement, substitution of charged residues should not affect the proportion of constitutively active channels. Therefore, they concluded that KCNE3 locks S4 in the active state.

We observed that in the presence of KCNE3 the C226 residue was always accessible, regardless of the membrane voltage (Fig. 5). This observation is also consistent with the idea that, within the KCNQ1–KCNE3 complex, the S4 segment is locked in the active state. But our finding that MTSES induces current increases in the presence of KCNE3 implies that the S4 segment is not completely locked in the active state. In addition, KCNQ1–KCNE3 channels still show voltage dependence that almost completely disappears after application of MTSES (Fig. 5, A and B). If C226 is always exposed to the extracellular milieu in the presence of KCNE3 and the accessibility is unchanged, regardless of membrane potential, the second order rate constant of the KCNQ1–KCNE3 A226C mutant should be as large as that of KCNQ1 or KCNQ1–KCNE1 during depolarization. And, indeed, the calculated second order rate constant was 0.025 ∼0.037 $s^{-1}mM^{-1}$, comparable to the apparent second order rate constant of KCNQ1–KCNE1 at 0 mV (0.031 ± 0.01 $s^{-1}mM^{-1}$; Fig. 4), which suggests that KCNE3 shifts the equilibrium of the S4 segment toward the active state, but does not necessarily lock it in the active state.

Concluding Remarks

Our MTS accessibility analysis revealed that the accessibility of C226 within the S4 segment is changed in the presence of KCNE1 or KCNE3. We interpret our results to indicate that the equilibrium between the resting and active states of the S4 segment is shifted by the presence of KCNE proteins; KCNE1 stabilizes S4 in the resting state, while KCNE3 stabilizes it in the active state. Future investigation will provide insight into the mechanisms by which KCNE auxiliary proteins accelerate or decelerate the transition of the S4 segment and where KCNE proteins interact with the S4 segment.

We thank Dr. T. Takumi (Osaka Bioscience Institute, Suita, Japan) for providing cDNA encoding rat KCNE1 and Dr. T. Hoshi (University of Pennsylvania, Philadelphia, PA) for human KCNQ1 cDNA. We thank Y. Asai for the preparation of oocytes and other technical assistance.

This work was supported by the research grants from the Ministry of Education, Culture, Sports, Science, and Technology of Japan to K. Nakajo (18790164) and to Y. Kubo, and from the Japan Society for the Promotion of Science to Y. Kubo.

Olaf S. Andersen served as editor.

Submitted: 18 April 2007
Accepted: 31 July 2007

REFERENCES

Abbott, G.W., F. Sesti, I. Splawski, M.E. Buck, M.H. Lehmann, K.W. Timothy, M.T. Keating, and S.A. Goldstein. 1999. MiRP1 forms I_{Kr} potassium channels with HERG and is associated with cardiac arrhythmia. *Cell.* 97:175–187.

Abbott, G.W., M.H. Butler, S. Bendahhou, M.C. Dalakas, L.J. Ptacek, and S.A. Goldstein. 2001. MiRP2 forms potassium channels in skeletal muscle with Kv3.4 and is associated with periodic paralysis. *Cell.* 104:217–231.

Akabas, M.H., D.A. Stauffer, M. Xu, and A. Karlin. 1992. Acetylcholine receptor channel structure probed in cysteine-substitution mutants. *Science.* 258:307–310.

Barhanin, J., F. Lesage, E. Guillemare, M. Fink, M. Lazdunski, and G. Romey. 1996. K_VLQT1 and lsK (minK) proteins associate to form the I_{Ks} cardiac potassium current. *Nature.* 384:78–80.

Bell, D.C., H. Yao, R.C. Saenger, J.H. Riley, and S.A. Siegelbaum. 2004. Changes in local S4 environment provide a voltage-sensing mechanism for mammalian hyperpolarization-activated HCN channels. *J. Gen. Physiol.* 123:5–19.

Gage, S.D., and W.R. Kobertz. 2004. KCNE3 truncation mutants reveal a bipartite modulation of KCNQ1 K^+ channels. *J. Gen. Physiol.* 124:759–771.

Gutman, G.A., K.G. Chandy, S. Grissmer, M. Lazdunski, D. McKinnon, L.A. Pardo, G.A. Robertson, B. Rudy, M.C. Sanguinetti, W. Stuhmer, and X. Wang. 2005. International Union of Pharmacology. LIII. Nomenclature and molecular relationships of voltage-gated potassium channels. *Pharmacol. Rev.* 57:473–508.

Isacoff, E.Y., Y.N. Jan, and L.Y. Jan. 1990. Evidence for the formation of heteromultimeric potassium channels in *Xenopus* oocytes. *Nature.* 345:530–534.

Kurokawa, J., H.K. Motoike, and R.S. Kass. 2001. TEA^+-sensitive KCNQ1 constructs reveal pore-independent access to KCNE1 in assembled I_{Ks} channels. *J. Gen. Physiol.* 117:43–52.

Larsson, H.P., O.S. Baker, D.S. Dhillon, and E.Y. Isacoff. 1996. Transmembrane movement of the shaker K^+ channel S4. *Neuron.* 16:387–397.

Ledwell, J.L., and R.W. Aldrich. 1999. Mutations in the S4 region isolate the final voltage-dependent cooperative step in potassium channel activation. *J. Gen. Physiol.* 113:389–414.

Long, S.B., E.B. Campbell, and R. Mackinnon. 2005. Crystal structure of a mammalian voltage-dependent Shaker family K^+ channel. *Science.* 309:897–903.

Mannuzzu, L.M., M.M. Moronne, and E.Y. Isacoff. 1996. Direct physical measure of conformational rearrangement underlying potassium channel gating. *Science.* 271:213–216.

Melman, Y.F., A. Domenech, S. de la Luna, and T.V. McDonald. 2001. Structural determinants of KvLQT1 control by the KCNE family of proteins. *J. Biol. Chem.* 276:6439–6444.

Melman, Y.F., A. Krumerman, and T.V. McDonald. 2002a. A single transmembrane site in the KCNE-encoded proteins controls the specificity of KvLQT1 channel gating. *J. Biol. Chem.* 277:25187–25194.

Melman, Y.F., A. Krummerman, and T.V. McDonald. 2002b. KCNE regulation of KvLQT1 channels: structure-function correlates. *Trends Cardiovasc. Med.* 12:182–187.

Melman, Y.F., S.Y. Um, A. Krumerman, A. Kagan, and T.V. McDonald. 2004. KCNE1 binds to the KCNQ1 pore to regulate potassium channel activity. *Neuron.* 42:927–937.

Panaghie, G., and G.W. Abbott. 2007. The role of S4 charges in voltage-dependent and voltage-independent KCNQ1 potassium channel complexes. *J. Gen. Physiol.* 129:121–133.

Panaghie, G., K.K. Tai, and G.W. Abbott. 2006. Interaction of KCNE subunits with the KCNQ1 K^+ channel pore. *J. Physiol.* 570:455–467.

Papazian, D.M., T.L. Schwarz, B.L. Tempel, Y.N. Jan, and L.Y. Jan. 1987. Cloning of genomic and complementary DNA from Shaker, a putative potassium channel gene from *Drosophila*. *Science.* 237:749–753.

Rocheleau, J.M., S.D. Gage, and W.R. Kobertz. 2006. Secondary structure of a KCNE cytoplasmic domain. *J. Gen. Physiol.* 128:721–729.

Ruppersberg, J.P., K.H. Schroter, B. Sakmann, M. Stocker, S. Sewing, and O. Pongs. 1990. Heteromultimeric channels formed by rat brain potassium-channel proteins. *Nature.* 345:535–537.

Sanguinetti, M.C., M.E. Curran, A. Zou, J. Shen, P.S. Spector, D.L. Atkinson, and M.T. Keating. 1996. Coassembly of K_VLQT1 and minK (IsK) proteins to form cardiac I_{Ks} potassium channel. *Nature.* 384:80–83.

Schroeder, B.C., S. Waldegger, S. Fehr, M. Bleich, R. Warth, R. Greger, and T.J. Jentsch. 2000. A constitutively open potassium channel formed by KCNQ1 and KCNE3. *Nature.* 403:196–199.

Schulze-Bahr, E., Q. Wang, H. Wedekind, W. Haverkamp, Q. Chen, Y. Sun, C. Rubie, M. Hordt, J.A. Towbin, M. Borggrefe, et al. 1997. KCNE1 mutations cause jervell and Lange-Nielsen syndrome. *Nat. Genet.* 17:267–268.

Seebohm, G., N. Strutz-Seebohm, O.N. Ureche, R. Baltaev, A. Lampert, G. Kornichuk, K. Kamiya, T.V. Wuttke, H. Lerche, M.C. Sanguinetti, and F. Lang. 2006. Differential roles of S6 domain hinges in the gating of KCNQ potassium channels. *Biophys. J.* 90:2235–2244.

Sesti, F., and S.A. Goldstein. 1998. Single-channel characteristics of wild-type I_{Ks} channels and channels formed with two minK mutants that cause long QT syndrome. *J. Gen. Physiol.* 112:651–663.

Smith-Maxwell, C.J., J.L. Ledwell, and R.W. Aldrich. 1998a. Role of the S4 in cooperativity of voltage-dependent potassium channel activation. *J. Gen. Physiol.* 111:399–420.

Smith-Maxwell, C.J., J.L. Ledwell, and R.W. Aldrich. 1998b. Uncharged S4 residues and cooperativity in voltage-dependent potassium channel activation. *J. Gen. Physiol.* 111:421–439.

Splawski, I., M. Tristani-Firouzi, M.H. Lehmann, M.C. Sanguinetti, and M.T. Keating. 1997. Mutations in the hminK gene cause long QT syndrome and suppress IKs function. *Nat. Genet.* 17:338–340.

Tai, K.K., and S.A. Goldstein. 1998. The conduction pore of a cardiac potassium channel. *Nature.* 391:605–608.

Tai, K.K., K.W. Wang, and S.A. Goldstein. 1997. MinK potassium channels are heteromultimeric complexes. *J. Biol. Chem.* 272:1654–1658.

Takumi, T., H. Ohkubo, and S. Nakanishi. 1988. Cloning of a membrane protein that induces a slow voltage-gated potassium current. *Science.* 242:1042–1045.

Takumi, T., K. Moriyoshi, I. Aramori, T. Ishii, S. Oiki, Y. Okada, H. Ohkubo, and S. Nakanishi. 1991. Alteration of channel activities and gating by mutations of slow ISK potassium channel. *J. Biol. Chem.* 266:22192–22198.

Tapper, A.R., and A.L. George Jr. 2000. MinK subdomains that mediate modulation of and association with KvLQT1. *J. Gen. Physiol.* 116:379–390.

Tapper, A.R., and A.L. George Jr. 2001. Location and orientation of minK within the I_{Ks} potassium channel complex. *J. Biol. Chem.* 276:38249–38254.

Timpe, L.C., T.L. Schwarz, B.L. Tempel, D.M. Papazian, Y.N. Jan, and L.Y. Jan. 1988. Expression of functional potassium channels from Shaker cDNA in *Xenopus* oocytes. *Nature.* 331:143–145.

Vemana, S., S. Pandey, and H.P. Larsson. 2004. S4 movement in a mammalian HCN channel. *J. Gen. Physiol.* 123:21–32.

Wang, H.S., Z. Pan, W. Shi, B.S. Brown, R.S. Wymore, I.S. Cohen, J.E. Dixon, and D. McKinnon. 1998. KCNQ2 and KCNQ3 potassium channel subunits: molecular correlates of the M-channel. *Science.* 282:1890–1893.

Wang, K.W., K.K. Tai, and S.A. Goldstein. 1996a. MinK residues line a potassium channel pore. *Neuron.* 16:571–577.

Wang, Q., M.E. Curran, I. Splawski, T.C. Burn, J.M. Millholland, T.J. VanRaay, J. Shen, K.W. Timothy, G.M. Vincent, T. de Jager, et al. 1996b. Positional cloning of a novel potassium channel gene: KVLQT1 mutations cause cardiac arrhythmias. *Nat. Genet.* 12:17–23.

Yang, N., A.L. George Jr., and R. Horn. 1996. Molecular basis of charge movement in voltage-gated sodium channels. *Neuron.* 16:113–122.

Yang, Y., and F.J. Sigworth. 1998. Single-channel properties of I_{Ks} potassium channels. *J. Gen. Physiol.* 112:665–678.